On the Upper Oceanic Heat Budget in the South China Sea: Annual Cycle①

Yang Haijun (杨海军), Liu Qinyu (刘秦玉) and Jia Xujing (贾旭晶)

Institute of Physical Oceanography, Ocean University of Qingdao, Qingdao 266003,

(Received December 12, 1998, revised January 11, 1999)

ABSTRACT

The upper oceanic heat budget in the South China Sea (SCS) is studied on the basis of ocean surface heat flux, upper sea heat storage and horizontal oceanic heat transport calculated from Comprehensive Ocean and Atmosphere Data Set. Several useful conclusions can be obtained and they are helpful for us to understand the climatologically thermal condition in the SCS. The annual variation of net heat budget reflects the adjustment and sudden change of the monsoon circulation over the SCS. The variation of upper oceanic heat storage of the SCS is tightly connected with the oceanic heat transport as well as the vertical movement in the SCS and so on.

Key words: South China Sea, Heat flux, Heat storage, Net heat budget

1. Introduction

In recent years the South China Sea (SCS) has become one of the most important regions in the local air–sea interaction research because of its special geographic position and semi–enclosed deep basin characteristics. The importance of the SCS is embodied mainly in which is one of the key heat and moisture sources of atmospheric circulation in eastern Asia. The onset and maintenance of the SCS monsoon are closely connected with the large heat transport from the SCS to air (Yan, 1997). The study on spatial–temporal variation of air–sea heat exchange in the SCS can help us not only enlighten the thermal structure of the SCS itself, but also properly estimate the potential ability of the influence of the SCS on atmospheric circulation in eastern Asia. In addition, reasonable underlying surface condition, especially the air–sea heat flux, has much effect on the model results in climatic prediction model.

In order to get a clearer understanding on the SCS thermal situation, we analyzed the seasonal and annual average heat budget components, and calculated the upper heat storage of the SCS. We also obtained the seasonal and annual average oceanic horizontal heat transport and upper vertical motion. The results are corresponding well to the distribution of temperature climatology.

2. Data and calculation methods

In this paper we use SST, surface air temperature, surface air pressure, surface scalar

①This work is supported by the Space–time Structure of South China Sea Circulation and Its Formation Mechanism(49636230) of the National Natural Science Foundation of China.

wind, air specific humidity and total cloudiness data, which are obtained from the Comprehensive Ocean and Atmosphere Data Set (COADS). The dataset includes monthly $2^\circ \times 2^\circ$ (latitude × longitude) data from 1950 to 1995. In order to get climatological monthly and annual mean heat flux, these data are averaged climatologically. In addition, we use the temperature data at 19 standard oceanographic analysis levels released by the National Oceanographic Data Center (Levitus, et al., 1994c) to calculate the upper heat storage of the SCS. Here the calculation region ranges from Equator to 24°N and from 100°E to 122°E. The seasons were defined as follows: December–February for winter, March–May for spring, June–August for summer and September–November for fall.

The surface net heat budget Q_{net} is defined as,

$$Q_{\rm net} = Q_{\rm sw} - Q_{\rm lw} - Q_{\rm lat} - Q_{\rm sen}, \tag{1}$$

where $Q_{\rm sw}$ and $Q_{\rm lw}$ are the heat due to solar short wave radiation and long wave radiation respectively, $Q_{\rm lat}$ is the latent heat flux and $Q_{\rm sen}$ the sensible heat flux. Readers can refer to Reed (1976, 1977), Kraus (1972) and Budyko (1956) to get these heat components. The surface net heat gain $Q_{\rm net}$ can also be written as (Hastenrath, et al. 1980),

$$Q_{\rm net} = Q_v + Q_t, \tag{2}$$

where Q_v is the divergence of oceanic horizontal heat transport, Q_t the upper oceanic heat storage anomaly to the annual mean value, which is estimated within the upper ten layers and the maximal depth is 200 m. For the long-term annual mean, Q_t can be assumed as zero (please refer to Section 3.3 for details).

3. The oceanic heat budget in the SCS

Based on estimate of the order of the heat budget components, we focus on the discussions of the seasonal and annual average patterns of the surface net radiation $R_{\rm net}$ (defined as the difference between $Q_{\rm sw}$ and $Q_{\rm lw}$), the total heat transport from sea to air $Q_{\rm sum}$ (defined as the sum of $Q_{\rm lat}$ and $Q_{\rm sen}$) and the surface net heat gain $Q_{\rm net}$.

3.1 *Mean seasonal patterns*

Figure 1 is the distributions of surface net radiation, total heat transport and surface net heat gain of the SCS in winter and summer. In the northern SCS the contours of net radiation in winter (Fig. 1a) are east–west alignment and nearly parallel to latitude, but they run from northeast to southwest in the south. The net radiation decreases gradually from south to north and its minimum is about 70 W • m^{-2}, which is located along the southeast coast of China mainland in the northern SCS. It is the annual minimum also. The maximum (about 160 W • m^{-2}) is in the west of Palawan Island and the Gulf of Thailand, which is more than two times of that in the north. The zonal pattern of net radiation and its large meridional difference are mainly due to the zonal distribution of the direct solar radiation from cloudless sky. Though zonal inhomogeneity of cloud cover produces the meridional difference of net radiation to some extent, monotonous atmosphere system over the SCS and low SST slow down the activity of air convection and then, lower the influence of cloud cover on the surface net radiation.

The surface net radiation in summer (Fig. 1b) is remarkably different from that in winter. Since the whole SCS is nearly between Equator and the Tropic of Cancer, the incident sunlight is practically vertical to the sea surface. It increases the short wave radiation greatly

absorbed by sea surface and makes the distribution of net radiation homogeneous, in other words, reduces its meridional difference (the maximal difference from south to north is only 30 W • m^{-2}). But here we should note that the surface net radiation does not obey zonal distribution any longer because of more air convection in summer.

The pattern of total heat transport Q_{sum} in winter (Fig. 1c) is almost opposite to that of surface net radiation. From south to north, Q_{sum} increases slowly and then grows sharply to the north of 18°N. Q_{sum} reaches maximum (beyond 30 W • m^{-2}) in the Luzon Strait and its west, which is far more than the absorbed short wave radiation in the same region and during the same period. We know that the surface wind and the air humidity are the most important factors to control latent heat transport (i.e., Q_{sum}). In winter, the northwest monsoon dominating the SCS brings cold and dry air, which has high potential to hold vapor, from higher latitude into the SCS continuously. It can cause a large amount of evaporation in the northern SCS. The cold and dry air mass will transform into warm and wet air with its southward movement, and this will repress the sensible and latent heat transport in the southern region. So Q_{sum} reduces from north to south. In addition, there is another factor being helpful for the large heat transport in the northern region, that is, the Kuroshio to the east of Luzon Island can form an anticyclonic loop when it flows nearby the Luzon Strait (Liu et al., 1996). The

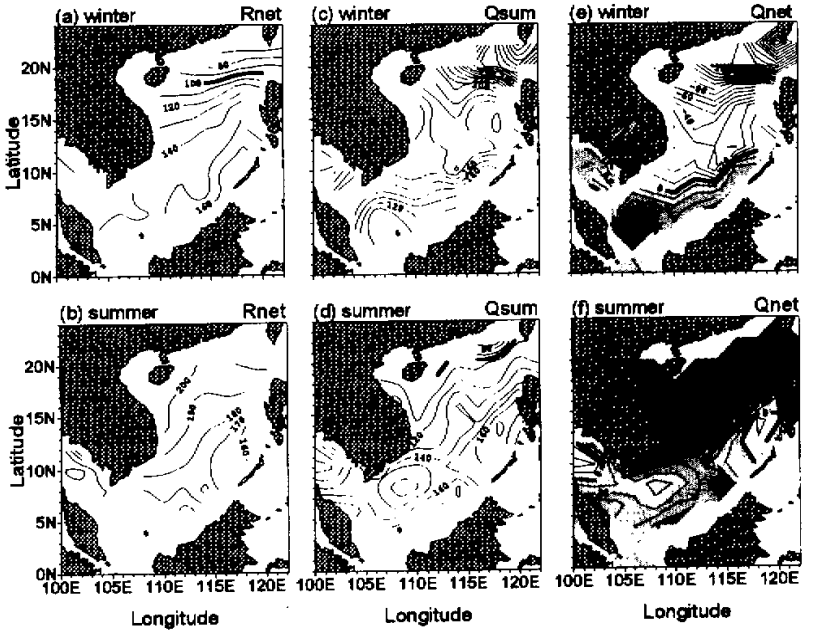

Fig. 1. Seasonal patterns of surface net radiation (R_{net}), total heat transport (Q_{sum}) and net surface heat gain (Q_{net}) for the South China Sea. (a) and (b) are for R_{net} in winter and summer respectively, (c) and (d) for Q_{sum}, (e) and (f) for Q_{net}. Contour interval is 10 W • m^{-2} and areas with $Q_{net} > 0$ are shaded in (e) and (f).

westward extent of the anticyclonic loop and even the detachment of warm vortex out of the main body of the Kuroshio can bring high temperature water into the northern SCS, and enlarge the difference of air–sea temperature, so does the heat transport from sea to air.

In summer the total heat transport is less and more homogenous than that in winter (Fig. 1d). The heat transport is high from the west of Luzon Island to Palawan Island, which maximum is about 160 W • m^{-2} and related to the high SST there. The minimal value 70 W • m^{-2} is along the coast of Guangdong Province of China in the northern SCS. Though there is strong southwest monsoon over the SCS, little evaporation of water restrained by the warm and wet air as well as small difference of air–sea temperature results less sensible and latent heat transport in summer than that in winter.

Now it is easy to obtain the surface net heat gain Q_{net} after we analyzed the net radiation and total heat transport in winter and summer. In winter (Fig. 1e) the surface loses heat except that to the south of 10°N. Due to the zonal distribution of R_{net}, the pattern of Q_{net} is mainly determined by that of Q_{sum}. The maximal net heat loss, which reaches −240 W • m^{-2}, occurs in the Luzon Strait and its west also, while the maximal heat gain in the south is only 40 W • m^{-2}. In summer (Fig. 1f) the surface net radiation exceeds the total heat transport from sea to air because of the increase of the absorbed short wave radiation, and the SCS gains heat almost everywhere. The surface net heat gain increases gradually from south to north.

From Eq. (2) we know that the surface net heat gain Q_{net} is balanced by two ways: one is the divergence of oceanic horizontal heat transport, the other is to change the upper oceanic heat storage. In winter, the oceanic heat can be transported from south to north along the north coast of Borneo Island and the west of Palawan Island continuously by the cyclonic circulation so as to compensate the heat loss in the north. Moreover, the intrusion of Kuroshio into the SCS can partly make up the northern heat loss (Guo et al., 1988).

Here we discuss the annual variations of surface net radiation, total heat transport and surface net heat gain. Fig. 2 is the annual varying curves of heat budget components for the SCS. We find that the solar short wave radiation Q_{sw} reaches maximum in April (more than 220 W • m^{-2}) because of the least cloud cover and the vertical incident of sunlight into surface. In May, Q_{sw} decreases much and it reflects the influence of more cloud cover. In winter Q_{sw} is lowest and less than 180 W • m^{-2}. But in general, the annual amplitude of Q_{sw} (defined as the difference of annual maximum and minimum) is not too large due to the tropical position of the SCS. Corresponding to the strong northeast monsoon and the cold and dry air, the latent heat transport Q_{lat} reaches maximum in winter, and lowers to the minimum in April, but increases rapidly after May and reaches another maximum in August, then a relatively minimum in September. The appearances of two maxima and two minima are tightly related to the establishment of northeast monsoon and southwest monsoon and the transition between them over the SCS. As a result, the surface net heat gain Q_{net} reaches maximum in April, drops quickly in May and keeps negative from October to next February. The varying trend of Q_{net} shows that the SCS gains heat for annual average though it loses heat seriously in winter. The SCS can store a large amount of heat energy so that it would exert remarkable influence on the atmospheric circulation and synoptic systems in eastern Asia. The sudden

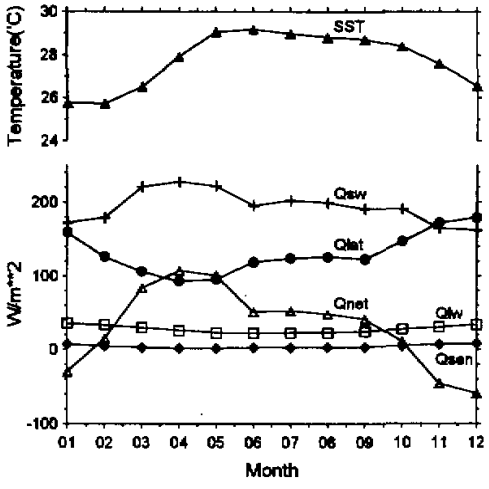

Fig. 2. Annual variations of oceanic heat budget components ($W \cdot m^{-2}$) and sea surface temperature(°C) averaged for the South China Sea. See text for further explanations.

change of Q_{sw}, Q_{lat}, Q_{net} in April–May reflects the quickly adjustment of atmospheric circulation before the onset of southwest monsoon over the SCS. The SCS act as a source of heat and vapor to maintain the monsoon. It is the water evaporation and convective heating caused by the strong air–sea interaction that influence the local synoptic systems over the SCS as well as the synoptic situation in China, Japan and even farther regions (Yan, 1997).

The annual variation of SST in the SCS is also given in Fig. 2. SST is the lowest in winter and rises swiftly after February. The maximal SST does not appear in April while the surface net heat gain reaches maximum but lags by about one to two months. Then the SST drops with the decrease of Q_{net}. Its annual amplitude is about 4°C. This implies that it is the surface net heat gain Q_{net} that decides the SST variation in the SCS.

3.2 *Annual average patterns*

Figure 3 is the annual patterns of surface net heat radiation R_{net}, total heat transport Q_{sum} and surface net heat gain Q_{net}. The annual average contour of R_{net} is nearly parallel to the latitude, which is very homogeneous in the SCS and the maximal difference from south to north is only 30 $W \cdot m^{-2}$. The pattern of Q_{sum} is much irregular, which is almost invariable to the south of 10°N but exceeds 200 $W \cdot m^{-2}$ in the Luzon Strait. We have introduced the influence of monsoon to analyze the seasonal variation of Q_{sum}, but for annual average the monsoon can be dismissed. The constant existence of the anticyclonic loop of the Kuroshio in the Luzon Strait makes the difference of air–sea temperature keep relatively high, so the annual average Q_{sum} is large. In turn it intensifies the convective activity of atmosphere, increases cloud cover and results in the small R_{net}. The final result is that annual average Q_{net} is negative, that is, this sea region is an important heat source and exports heat to air throughout a year, while the region to the south of 18°N is a huge heat sink.

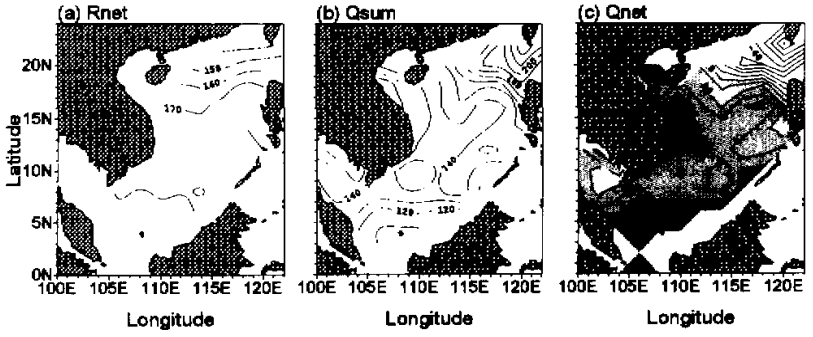

Fig. 3. Annual average patterns of (a) surface net radiation (R_{net}), (b) total heat transport (Q_{sum}) and (c) net surface heat gain (Q_{net}) for the South China Sea during 1950–1995. Contour interval is 10 W • m^{-2} and areas with $Q_{net} > 0$ are shaded in (c).

3.3 *Upper oceanic heat storage*

We use the following equation to calculate the upper oceanic heat storage anomaly Q_t in the SCS (Levitus, 1984):

$$Q_t = \frac{\rho_0 C_p}{t} \sum_{k=1}^{K_{max}} (\overline{T}_{season} - \overline{T}_{annual}) \cdot \Delta Z_k , \tag{3}$$

where k represents standard level number, K_{max} the deepest standard level, which is set as 10 in this paper, that is, the integration is performed from surface to 200 m in depth. The density of sea water ($\rho_0 = 1.025 \times 10^3 kg \cdot m^{-3}$ and the specific heat of sea water $C_p = 4187\ J \cdot kg^{-1} \cdot K^{-1}$, t the three months in unit of seconds, $\overline{T}_{season}$ the seasonal average temperature, $\overline{T}_{annual}$ the annual average temperature. Eq.(3) shows that the heat storage variability is decided by the difference between seasonal average temperature and annual average temperature. The depth interval ΔZ_k is 5 m for the sea surface and $\Delta Z_k = (Z_{k+1} - Z_{k-1})/2$ for all other standard levels. The depth of each standard level is given by Levitus (1982, Table 1).

Figure 4 is the seasonal average latitudinal variation of Q_t in the SCS. We find that the meridional variation of Q_t in winter and spring is almost out of phase with those in summer and fall. In winter Q_t drops linearly from south to north except that it is positive to the south of 2°N, which minimum is in the northern SCS. From the analyses to Fig. 1, we know the SCS loses heat in winter. The cold and dry air brought by northeast monsoon increases the heat transport from sea to air and causes the temperature in upper sea to drop rapidly. Then the upper mixing layer is thickened by means of convective and turbulent mixing and its average temperature reaches annual minimum. Accordingly, the upper oceanic heat storage reduces greatly. In summer, the warm and wet air brought by southwest monsoon restrains the convective mixing in upper sea, prevents the heat loss from lower water. At the same time, the upper water is heated by the way of radiation transfer. So Q_t increases and its meridional variation is the same as that of Q_{net} in summer, which reaches maximum (75 W • m^{-2}) in the northern SCS.

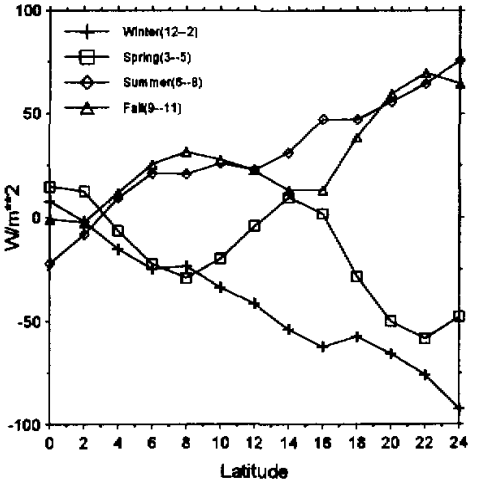

Fig. 4. Seasonal average latitudinal variations of upper oceanic heat storage ($W \cdot m^{-2}$) of the South China Sea (100–122°E). See text for further explanations.

There are two maxima and two minima in the meridional variation of Q_t in spring and fall respectively. Though the surface wind velocity decreases and net radiation increases in spring, the average temperature in the upper water rises slowly due to oceanic thermal–inertia. From above we have known that the maximum SST lags Q_{net} by about one to two months, so the temperature in upper sea is still below the annual average value. Here we should pay special attention to the maximum Q_t near 14°N. It is the reflection of the SCS warm pool, which is a large warm water mass appearing in the central SCS and the west of Luzon Island in early April. The maximal SST of the SCS warm pool is nearby the band of 12°N. The appearance of the SCS warm pool is the most obvious manifestation of local air–sea interaction. Since there is always a high air pressure over the central SCS in late winter and early spring the downward motion in the central high pressure represses the sensible and latent heat transport from sea surface, reduces cloud cover, that is, increases the solar short wave radiation absorbed by surface. At the same time, the anticyclonic wind produces anticyclonic circulation in the sea and drives the surface warm water to converge to the center of circulation. So the downwelling in the sea occurs and causes the upper water temperature to rise quickly (Chu et al., 1997). As a result, the upper oceanic heat storage increases rapidly. As to why the minimum Q_t appears at the same latitude (14°N) in fall, it may be also connected with the strongest air–sea interaction there.

3.4 *Meridional oceanic heat transport*

The meridional heat transport within the ocean can be obtained by integrating Q_v over latitude bands (Hastenrath et al., 1980). Connecting Eqs.(2) and (3) we can get the seasonal average Q_v, Q_v is equal to Q_{net} in the case of annual average. The meridional heat transport (MHT) can be written as

$$H_{\mathrm{mt}}(\varphi)=\int_{\varphi_0}^{\varphi}\int_{\lambda_0}^{\lambda_1} Q_v(\lambda,\varphi)R_e^2\cos\varphi\, d\lambda d\varphi, \tag{4}$$

Here, φ is latitude and $\varphi_0 = 0$ represents Equator, λ_0 and λ_1 are longitude which are given as 100°E and 122°E respectively, R_e the radius of the Earth. Because the Karimata Strait in the southern SCS is very shallow and the meridional current there is weak, we assume that the MHT through this strait is equal to zero, that is, $H_{\mathrm{mt}}(\varphi_0)= 0$ as the boundary condition of integration. This has no essential influence on the heat transport in the SCS.

Figure 5 is the seasonal and annual average net MHT. The MHT in all seasons is northward except that to the north of 16°N in fall. In winter the maximum northward MHT occurs at 16°N and, to the north the northward transport decreases gradually. It implies that there is heat convergence in the northern SCS in winter. In spring the northward MHT increases linearly from south to north and the amount of MHT is far more than that of other seasons, which reaches maximum at the north end of the SCS. The increase of MHT is primarily due to the increase of short wave radiation absorbed by sea surface. In summer and fall the northward MHT is relatively small. Southward MHT appears to the north of 16°N in fall.

We note that there is no simple linear relationship between the heat transport and upper water temperature. Even that the Q_{net} is negative in certain sea region, the water can still attain the aim to export heat by means of reducing the heat storage itself. On the contrary, even certain region gains much heat, but if its gain is mainly used to increase heat storage itself, then the heat export will be little. In addition, the oceanic circulation corresponding to the monsoon can determine the direction of heat transport to a great extent. This is why the northward MHT is much in winter and spring and little in summer and fall.

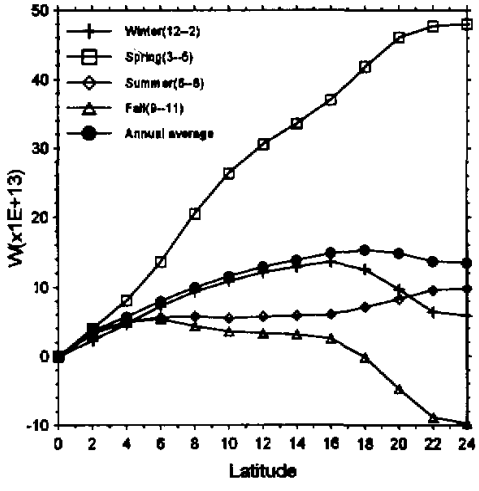

Fig. 5. Seasonal and annual average net meridional heat transport(10^{13}W) in the South China Sea (100–122°E). Northward transport is positive. See text for further explanations.

For annual average the MHT is northward always. The northward MHT reaches maximum at 18°N, and reduces slightly between 18–24°N. In Section 3.2 we have known that in the northern SCS the annual average heat of the upper ocean loses, that is, there is heat convergence in order to maintain the heat export to air, but we find the meridional heat supply is not much enough (about 1.93×10^{13}W). It implies that there may be zonal heat convergence, that is, the Kuroshio may transport heat to the SCS through the Luzon Strait.

4. Vertical movement in the SCS

For steady–state conditions, the divergence of oceanic horizontal heat transport is related to the vertical motion in the upper sea by (Wyrtki, 1965; Hastenrath et al., 1980)

$$W_h = \frac{Q_v}{\rho_0 C_p \Delta T}, \tag{5}$$

where ρ_0, C_p are as before, temperature difference $\Delta T = T_{\text{surface}} - T_{\text{bottom}} > 0$, defined as the difference of SST and the temperature at the depth of 200 m. W_h is the average vertical velocity in the upper layer. $W_h > 0$ when $Q_v > 0$, that is, upwelling occurs to maintain the oceanic thermal structure.

Figure 6 shows the average vertical motion in winter and summer and in the case of annual average. Downwelling occurs to the north of 18°N in winter(Fig. 6a) due to the heat convergence. To the south of 18°N, upwelling dominates the southeastern SCS. The maximum with a value in excess of 20×10^{-7}m • s^{-1} lies to the west of Luzon Island, which is exact the position of Luzon cold eddy (LCE) (Yang et al., 1998). The LCE is a semi–permanent cold cyclone located to the west of Luzon Island in winter and spring and its existence has been proved by many studies (Zeng et al., 1989; Shaw et al., 1996). However, its formation mechanism has not been well explained. We find the LCE again from the point of view of heat transport. It suggests that the heat divergence in this region is maintained by the water vertical motion during winter.

The upper oceanic vertical motion in summer (Fig. 6b) is almost opposite to that in winter. The maximum downwelling appears to the west of Luzon Island at this time. Upwelling

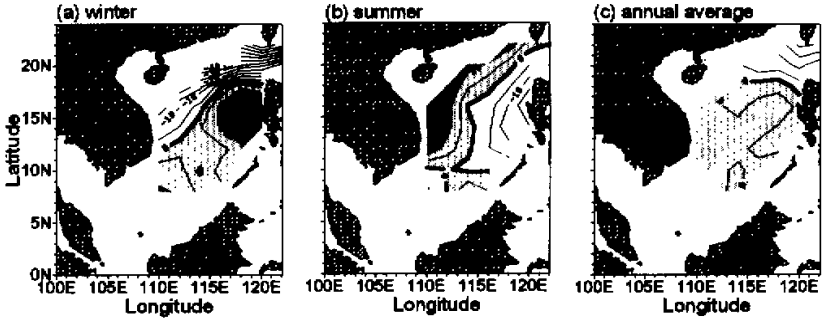

Fig. 6. Seasonal and annual average oceanic vertical motion in the upper South China Sea. (a) is for winter, (b) for summer and (c) for annual average. Upward motion is positive and shaded. Contour interval is 5×10^{-7}m • s^{-1}.

occurs in the continental shelf and slope of the SCS as well as the eastern coast of Vietnam. The maximum upwelling is along the coast of Vietnam, which is corresponding to another cyclonic eddy—the Vietnam cold eddy (VCE) (Yang et al., 1998). The pattern of upwelling in the west and downwelling in the east of the SCS implies that the oceanic heat is transported not only from south to north, but also from west to east. It might be restrained by zonal vertical circulation probably existed in summer. In the case of annual average, there is upwelling to the south of 18°N and downwelling to the north. The vertical velocity is small since the remarkably seasonal difference is smoothed by annual average. The downwelling in the northern SCS is due to the heat import from the Kuroshio, which has been analyzed in Fig. 5 before.

5. Conclusions

The analyses above give us a way to understand the climatological state of the surface net heat budget, the upper oceanic heat storage, the meridional heat transport and the vertical motion in the upper SCS, as well as the complex relation between them. We can obtain the following conclusions:

(1) The surface loses heat to the north of 10°N of the SCS and gains heat to the south in winter. In summer the surface gains heat in the SCS as a whole. (2) The surface net heat gain reaches maximum in April and decreases rapidly after May. It keeps negative from October to next February. (3) The annual average surface net heat budget is negative to the north of 18°N and positive to the south. (4) The upper oceanic heat storage of the SCS is negative in winter and spring and positive in summer and fall. Its meridional variation in wintertime is approximately out of phase with that in summertime. (5) The seasonal and annual average meridional oceanic heat transport are always northward except that to the north of 16°N in fall. (6) There is upwelling to the south of 18°N and downwelling to the north in the SCS in winter. In summer the upper vertical motion is almost opposite to that in winter. Downwelling occurs to the west of Luzon Island and upwelling in the continental shelf and slope region and also along the east coast of Vietnam. In the case of annual average, upwelling occurs to the south of 18°N and downwelling to the north but the velocity is small.

The variation of the surface net heat budget usually leads that of sea temperature, and it can be viewed as a useful index to understand the oceanic thermal and dynamic structure. For example, the positive heat budget always implies that the upper sea temperature would rise in the near future. And at the same time, the oceanic current would be changed to adapt the oceanic thermal state or change the thermal distribution in turn. In above study, the oceanic regime is actually assumed as quasi–steady. So, in the sense of long–term average, the results we obtain are reasonable.

REFERENCES

Budyko, M.I., 1956: *The Heat Balance of the Earth's Surface* (in Russian). 255 pp., Gidrometeorol. Izd., St. Petersburg, Russia.

Chu, P.C., and Chang C. P., 1997: South China Sea warm pool in boreal spring. *Adv. Atmos. Sci.*, **14**, 195–206.

Guo, Z.X., and Fang W. D., 1988: The Kuroshio in Luzon Strait and its transport during September 1985. *Tropic Oceanology* (in Chinese), **2**, 13–19.

Hastenrath, S., and J. L. Peter, 1980: On the heat budget of hydrosphere and atmosphere in the Indian Ocean. *J. Phys. Oceanogr.*, **10**, 694–708.

Kraus, E. B., 1972: *Atmospheric–Ocean Interaction*, 275pp., Oxford Univ. Press, New York.

Levitus, S., 1982: Climatological Atlas of the World Ocean. NOAA Prof. Pap. No.13, U.S. Government Printing Office, Washington, DC, 173 pp.

Levitus, S., 1984: Annual cycle of temperature and heat storage in the world ocean. *J. Phys. Oceanogr.*, **14**, 727–746.

Levitus, S., and T. P. Boyer, 1994c: World Ocean Atlas 1994 Volume 4: Temperature. NOAA Atlas NESDIS 4, 177pp.

Liu, Q. Y., Liu Z. T., et al, 1996: The Deformation of Kuroshio in the Luzon Strait and its Dynamics. *J. Ocean University of Qingdao* (in Chinese), **26(4)**, 413–419.

Reed, R. K., 1976: On estimation of net long–wave radiation from the oceans. *J. Geophys. Res.*, **81(33)**, 5793–5794.

Reed, R.K., 1977: On estimating insolation over the ocean. *J. Phys. Oceanogr.*, **7**, 482–485.

Shaw, P.T., Chao S. Y., Liu K. K., Pai S. C., and Liu C. T., 1996: Winter upwelling off Luzon in the northeastern South China Sea. *J. Geophys. Res.*, **101**, 16435–16448.

Wyrtki, K., 1965: The average annual heat balance of the North Pacific Ocean and its relation to ocean circulation. *J. Geophys. Res.*, **70**, 4547–4559.

Yan, J. Y., 1997: Observational study on the onset of the South China Sea southwest monsoon. *Adv. Atmos. Sci.*, **14**, 275–287.

Yang, H. J., and Liu Q. Y., 1998: The seasonal features of temperature distributions in the upper layer of the South China Sea. *Oceanologia et limnologia Sinica*, **29**, 501–507.

Zeng, Q. C., Li R. F., Ji Z., Gan Z., and Ke P., 1989: Calculation of the monthly mean circulation in the South China Sea. *Scientia Atmospherica Sinica* (in Chinese), **13**, 127–168.